Functionalized thermosensitive hydrogel combined with tendon stem/progenitor cells as injectable cell delivery carrier for tendon tissue engineering

To cite this article: Heyong Yin *et al* 2018 *Biomed. Mater.* **13** 034107

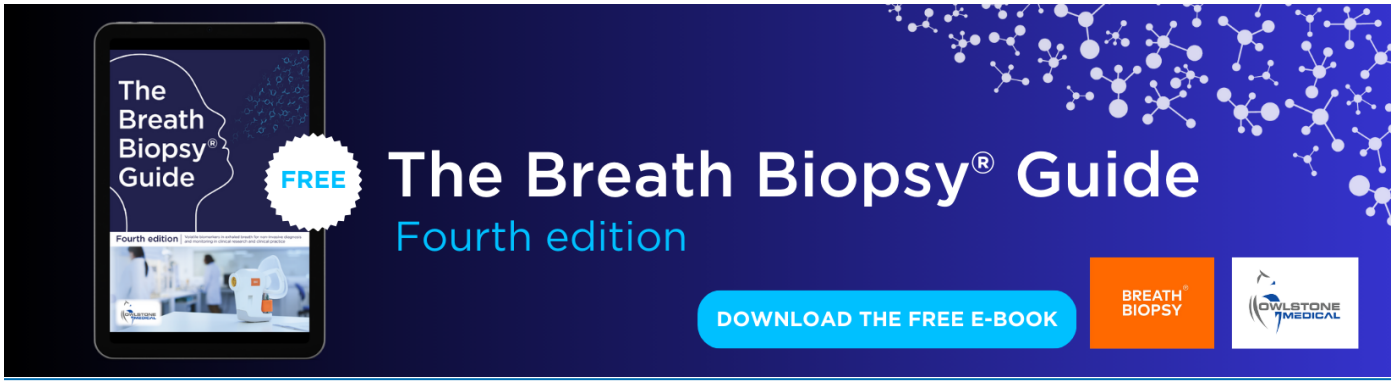

Biomedical Materials

PAPER

Functionalized thermosensitive hydrogel combined with tendon stem/progenitor cells as injectable cell delivery carrier for tendon tissue engineering

Heyong Yin[1,2,3], **Zexing Yan**[2], **Richard J Bauer**[4], **Jiang Peng**[3], **Matthias Schieker**[1,5], **Michael Nerlich**[2] **and Denitsa Docheva**[2,6,7]

[1] Experimental Surgery and Regenerative Medicine, Department of Surgery, Ludwig-Maximilians-University (LMU), Munich, Germany
[2] Experimental Trauma Surgery, Department of Trauma Surgery, University Regensburg Medical Centre, Regensburg, Germany
[3] Institute of Orthopaedics, Key Laboratries of Regenerative Medicine in Orthopaedics and Musculoskeletal Trauma & War Injuries, Chinese People's Liberation Army General Hospital, Beijing, People's Republic of China
[4] Department of Oral and Maxillofacial Surgery and Center for Medical Biotechnology at Biopark I, University Regensburg Medical Centre, Regensburg, Germany
[5] Novartis Institutes for Biomedical Research (NIBR), Translational Medicine Musculoskeletal Disease, Basel, Switzerland
[6] Department of Medical Biology, Medical University-Plovdiv, Plovdiv, Bulgaria
[7] Author to whom any correspondence should be addressed.

E-mail: Heyong.Yin@ukr.de, Zexing.Yan@ukr.de, Richard.Bauer@ukr.de, Pengjdxx@126.com, Matthias.Schieker@med.uni-muenchen.de, Michael.Nerlich@ukr.de **and** Denitsa.Docheva@ukr.de

OPEN ACCESS

RECEIVED
15 November 2017

REVISED
1 February 2018

ACCEPTED FOR PUBLICATION
8 February 2018

PUBLISHED
16 March 2018

Keywords: tendon stem/progenitor cell, tendon repair, tissue engineering, thermosensitive hydrogel

Supplementary material for this article is available online

Abstract

Thermosensitive hydrogels have been studied for potential application as promising alternative cell carriers in cell-based regenerative therapies. In this study, a thermosensitive butane diisocyanate (BDI)-collagen hydrogel (BC hydrogel) was designed as an injectable cell delivery carrier of tendon stem/progenitor cells (TSPCs) for tendon tissue engineering. We functionalized the BDI hydrogel with the addition of 20% (v/v) collagen I gel to obtain the thermosensitive BC hydrogel, which was then seeded with TSPCs derived from human Achilles tendons. The BC hydrogel compatibility and TSPC behavior and molecular response to the 3D hydrogel were investigated. Collagen (COL) I gel served as a control group. Our findings demonstrated that the BC hydrogel was thermosensitive, and hardened above 25 °C. It supported TSPC survival, proliferation, and metabolic activity with satisfactory dimension stability and biocompatibility, as revealed by gel contraction assay, live/dead staining, DNA quantification, and resazurin metabolic assay. Phalloidin-based visualization of F-actin demonstrated that the TSPCs were stretched within COL I gel with classical spindle cell shapes; similar cell morphologies were also found in the BC hydrogel. The gene expression profile of TSPCs in the BC hydrogel was comparable with that in COL I gel. Moreover, the BC hydrogel supported capillary-like structure formation by human umbilical vein endothelial cells (HUVECs) in the hydrogel matrix. Taken together, these results suggest that the thermosensitive BC hydrogel holds great potential as an injectable cell delivery carrier of TSPCs for tendon tissue engineering.

1. Introduction

Tendon injuries present great challenges in orthopedic and trauma surgery due to the high occurrence rate of sports- and age-related traumatic events, and it accounts for about 45% of all musculoskeletal injuries [1, 2]. Moreover, most of these injuries tend to become chronic conditions, and ruptured tendons rarely fully gain their initial strength and function [3–5]. Currently, there are numerous treatment options for repairing injured tendons, including conservative treatments (physiotherapy, active motion, anti-inflammatory medications) and surgical treatment (suturing, tissue autografts or allografts, tendon-to-bone fixation). But frequently, they do not dramatically improve long-term patient outcomes [6–8].

The prevalence of tendon and ligament injuries and the unsatisfactory long-term outcomes of the current therapeutic options are driving the need for

alternative treatment, with cell-based tissue engineering being one of the most attractive and widely explored strategies. Cell source is a critical element in tendon tissue engineering. TSPC was first identified by Bi Y *et al* [9] in 2007, and follow-up studies by independent research groups showed that it was a very promising reparative cell source for tendon repair [5, 10]. Our team has abundant research experience on TSPC, and well established and characterized TSPC donors derived from non-ruptured Achilles tendon biopsies of young and healthy patients undergoing lower extremity operations due to accidents [11–13].

The selection of a cell carrier is also a key factor to the success of cell-based tissue engineering approaches in tendon repair. Hydrogels, particularly thermosenstive hydrogels, have been extensively studied because they provide a 3D environment that support *in vitro* cell proliferation and matrix remodeling, and can serve as cell delivery vehicles for *in vivo* implantation [14]. Moreover, thermosensitive hydrogels can be injected *in vivo* as fluids to fill the desired tissue defect completely and form gels at body temperature with minimal invasion, and can incorporate various cells, drugs, and growth factors through simple mixing [15].

Pluronic is a thermosensitive synthetic polymer, which undergoes gelation above its critical solution temperature (LCST) [15, 16]. Multiple studies have shown that synthetic thermosensitive hydrogels like pluronic have promising characteristics as materials for tissue engineering; however, cell survival is not frequently satisfactory in hydrogels [17–19]. A previous study reported that modifying pluronic (P123) with chain extender butane diisocyanate (BDI) leads to a decrease of the polymer concentration necessary for micellization. The resulting thermosensitive BDI hydrogel (Europe patent number: WO2014095915A1) exhibited improved storage moduli, and pilot analyses with immortalized human mesenchymal stem cells (hMSCs) suggested cell survival up to 24 h but no obvious cell spreading in the hydrogel [16]. To further improve the biocompatibility of such materials, the addition of bioactive materials has been proposed. Park *et al* [15] and Khattak *et al* [18] applied chitosan and different membrane-stabilizing agents in order to functionalize pluronic hydrogels, and demonstrated significant improvement of cell attachment and proliferation.

COL I is the most abundant matrix protein in tendon tissues and is well-known for its good biocompatibility [20]. Furthermore, its nanofibrous structure and the presence of a GFOGER sequence, which is a high-affinity binding site for integrin receptors, strongly promote cell attachment and anchorage-dependent cell survival [21]. Therefore, in this study, we functionalized the BDI hydrogel with COL I to prepare a novel synthetic/natural hybrid BDI-collagen (BC) hydrogel. Pure COL I gel served as a control group in this work. We evaluated the hydrogels, BC versus COL I, in terms of how they affect TSPC behavior using gel contraction assay, cell morphology, survival, proliferation, gene expression and matrix organization analyses, as well as testing their vascular permeability.

2. Material and methods

2.1. Cell isolation and expansion

Human TSPCs from non-ruptured Achilles tendon biopsies derived from three young and healthy human patients were previously described and profoundly characterized by Kohler *et al* [11] with approval by the Ethical Commission of the LMU Medical Faculty (Ethical Grant No. 166-08). The three primary cell lines were abbreviated as Y1-TSPC, Y2-TSPC, and Y3-TSPC respectively. TSPCs were isolated according to Kohler *et al* [11]. Briefly, Achilles tendon tissue was minced into small pieces, digested with 0.15% collagenase II (Worthington, Lakewood, NJ, USA) over night in a 37 °C incubator, filtered with 100 μm pore size nylon mesh, and centrifuged for 10 min at 500 g. The cell pellet was then resuspended in DMEM/Ham's F-12 (1:1 mixture) supplemented with stabile glutamine, 1% MEM amino acids (Biochrom, Berlin, Germany), 10% FBS, and 1% L-ascorbic acid-2-phosphate (Sigma-Aldrich, Munich, Germany), and the TSPCs were maintained at a constant temperature of 37 °C under 5% CO2 humidified atmosphere. TSPCs at passage 3–6 were used in all experiments.

Human umbilical vein endothelial cells (HUVECs, Cat.#1210111, Provitro AG, Germany) were cultured in endothelial cell basal proliferation medium supplemented with 7% FCS, 1% heparin, 0.1% ascorbic acid, and 0.02% hydrocortisone (all from Provitro AG) in a humidified incubator at a constant temperature of 37 °C and 5% CO2. Cells at passage 3–6 were used in these experiments.

2.2. Casting gels with TSPCs

A BDI hydrogel was prepared as described previously by Volkmer *et al* [16]. First, 1 g BDI polymer was autoclaved, and diluted in 8 ml TSPC culture medium, mixed thoroughly to obtain a homogeneous hydrogel. Then, the BDI hydrogel was functionalized by adding 20% (v/v) COL I derived from rat tail tendons (LOT:354 236; Millipore), resulting in a synthetic/natural hybrid BC hydrogel which, prior to mixing with cells, was incubated overnight at −4 °C. Pure BDI and COL I hydrogels served as control groups. COL I gels were prepared according to the manufacturer's protocol at a final COL I concentration of 1.25 mg ml^{-1}. The pH was adjusted to 7.4 using 1 N NaOH (Sigma). For casting 3D hydrogels with cells, 3 Y-TSPC donors were encapsulated at a cell density of 6 × 104 cells/100 μl (6 × 10^2 mm^{-3}) in BDI, COL I or BC hydrogel. Once mixed thoroughly, 100 μl cell-gel mixture was pipetted into a sterile cylindrical mold

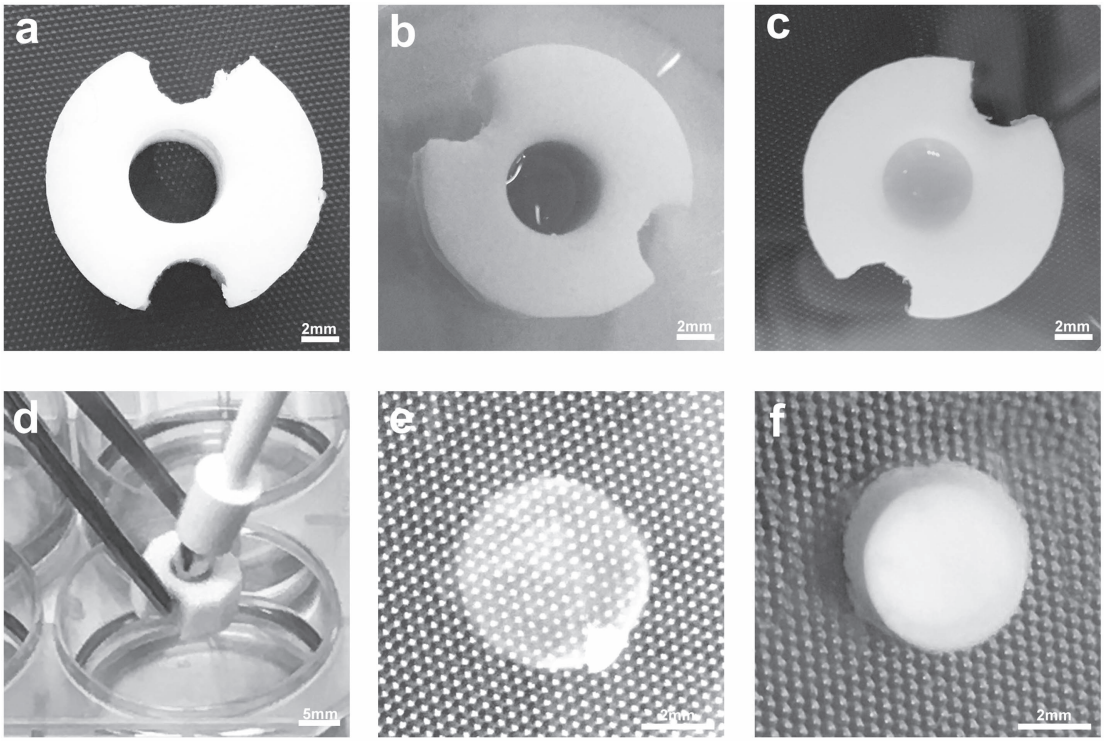

Figure 1. Casting gels. (a) Cylindrical mold 5 mm in diameter. (b) Filled with 100 μl gels. (c) Gelation at 37 °C incubation for 30 min. (d) Punching the gels out of the mould with a sterilized punch. Macroscopy images of COL I (e) and BC (f) hydrogels.

(5 mm in diameter and 5 mm in height), incubated at 37 °C for 30 min until gelation, and then punched out with a sterilized punch (figure 1). Next, the harvested cylindrical hydrogels (each 98 mm^3) were cultivated in culture medium and incubated at a constant temperature of 37 °C under 5% CO_2 humidified atmosphere. The gel area and weight were monitored over a period of 7 days. The analysis of the gel area at each time point was presented as a percentage of the initial gel size. The data consists of two independent experiments with all three donors in triplicates ($n = 6$).

2.3. Cell viability, apoptosis, and proliferation assays

Cell viability and proliferation were assessed by live/dead staining, DNA quantification, JC-1 staining, and resazurin cell metabolic assay.

For live/dead staining, the whole hydrogels were washed with PBS and then stained for 5 min at room temperature in 5 $\mu g\,ml^{-1}$ calcein AM and 5 $\mu g\,ml^{-1}$ ethidium homodimer-1 (Molecular probes, Eugene, Oregon). The DNA content was quantified using a PicoGreen DNA kit (Invitrogen, Carlsbad, CA) according to the manufacturer's protocol. A standard curve based on known DNA concentration was applied to determine the total cell DNA contents of the samples. To determine cell apoptosis in the hydrogels, JC-1 staining was performed as previously reported [22]. Briefly, after washing with PBS, the hydrogels were incubated in 5 mg ml^{-1} JC-1 dye for 30 min with shaking at 37 °C. Resazurin for the cell metabolic assay (Sigma-Aldrich) was performed according to the manufacturer's protocol.

Fluorescence images were taken with an Olympus XC10 camera on an Olympus BX61 fluorescence microscope (Olympus, Japan). Live/dead staining, DNA quantification, JC-1 staining, and resazurin assays were repeated independently twice with 3 Y-TSPC donors in triplicates ($n = 6$). Cell aspect ratio (width/length) (figure 4(b)) was analyzed using Image J (National Institutes of Health, Bethesda, MD, USA) to demonstrate cell elongation during cultivation in the hydrogels over a period of 7 days. Three donors per group, each represented by three images, were analyzed manually with an Image J measure tool at four different time points (day 0, 1, 3 and 7). The data was expressed as aspect ratio and represents the average of 90 cells/group.

2.4. RNA isolation and qPCR

The total RNA from the hydrogels with three TSPC donors was extracted using a Qiagen RNeasy Mini kit (Qiagen, Hilden, Germany) and used for qRT-PCR. For cDNA synthesis, 1 μ g total RNA and a Transcriptor First-Strand cDNA Synthesis Kit (Roche) were used. Quantitative PCR of tenogenic, lineage, and cross-linking gene markers, as listed in table 1, was performed using RealTime PCR Ready Custom design plates with format 96-well/32+ [8]according

[8] https://configurator. realtimeready.roche.com [(Accessed: 15 February 2018)].

Table 1. Genes from RealTime PCR Ready Custom designed plates analysed in this study.

Target gene	Abbreviation	Category
Asporin	ASPN	Tendon-related matrix gene
Tenomodulin	TNMD	Tendon-related matrix gene
Biglycan	BGN	Tendon-related matrix gene
Decorin	DCN	Tendon-related matrix gene
Fibromodulin	FMOD	Tendon-related matrix gene
Proteoglycan 4	PRG4	Tendon-related matrix gene
Lumican	LUM	Tendon-related matrix gene
Cartilage oligomeric matrix protein	COMP	Tendon-related matrix gene
Tenascin C	TNC	Tendon-related matrix gene
Thrombospondin 2	THBS2	Tendon-related matrix gene
Scleraxis homolog A	SCXA	Transcription factor gene
Mohawk homeobox	MKX	Transcription factor gene
Early growth response 1	EGR1	Transcription factor gene
Early growth response 2	EGR2	Transcription factor gene
Eyes absent homolog 1	EYA1	Transcription factor gene
Eyes absent homolog 2	EYA2	Transcription factor gene
SIX homeobox 1	SIX1	Transcription factor gene
SIX homeobox	SIX2	Transcription factor gene
Collagen type I alpha 1	COL1A1	Tendon-related collagen gene
Collagen type III alpha 1	COL3A1	Tendon-related collagen gene
Collagen type V alpha 1	COL5A1	Tendon-related collagen gene
Collagen type VI alpha 1	COL6A1	Tendon-related collagen gene
Collagen type XII alpha 1	COL12A1	Tendon-related collagen gene
Collagen type XIV alpha	COL14A1	Tendon-related collagen gene
Collagen type XV alpha 1	COL15A1	Tendon-related collagen gene
Fibronectin 1	FN1	Others
Actin alpha 2	ACTA2	Others
EPH receptor A4	EPHA4	Others
Transforming growth factor beta 1	TGFB1	Others
Lysyl oxidase	LOX	Collagen cross-linking gene
Transglutaminase 2	TGM2	Collagen cross-linking gene
Procollagen-lysine 5-dioxygenases	PLOD1	Collagen cross-linking gene
Sex determining region Y box 9	SOX9	Chondrogenic gene
Aggrecan	ACAN	Chondrogenic gene
Collagen type II alpha 1	COL2A1	Chondrogenic gene
Runt-related transcription factor 2	RUNX2	Osteogenic gene
Sp7 transcription factor	SP7	Osteogenic gene
Integrin-binding sialoprotein	IBSP	Osteogenic gene
Peroxisome proliferator-activated receptor gamma	PPARG	Adipogenic gene
Lipoprotein lipase	LPL	Adipogenic gene
Transcription factor AP-2 alpha	TFAP2A	Adipogenic gene
Myogenic differentiation 1	MYOD1	Myogenic gene
Myogenin	MYOG	Myogenic gene
Desmin	DES	Myogenic gene
Nanog homeobox pseudogene 8	NANOG	Embryonic gene
POU domain, class 5, transcription factor 1	POU5F1	Embryonic gene
Fucosyltransferase 4	FUT4	Embryonic gene
Glyceraldehyde-3-phosphate dehydrogenase	GAPDH	Reference gene

to the manufacturer's instructions (Roche, Penzberg, Germany). Briefly, PCR reactions were pipetted on ice and each well contained 10 μl LightCycler 480 probes master mix, 0.2 μl undiluted cDNA and 9.8 μl PCR grade water. Plates were subsequently sealed and centrifuged down for 15 s at 2100 rpm. The $\Delta\Delta$Ct method was used to analyze the qPCR results. Gene expression was calculated as fold change compared to COL I gel. The PCR results were attained with 3 Y-TSPC donors ($n = 3$).

2.5. Immunofluorescence and F-actin stainings

At day 3, hydrogel samples were fixed in 4% paraformaldehyde for 1 h at 37 °C and washed in PBS for 10 min. For immunofluorescence, the whole contacted gel was treated with 2 mg ml^{-1} hyaluronidase (Sigma-Aldrich, Steinheim, Germany) for 15 min at 37 °C for antigen retrieval. After washing and blocking with 1% bovine serum albumin (Sigma-Aldrich), primary antibodies against collagen I (Cat.#C2456, Sigma-Aldrich), collagen V (Cat.#ab114072, Abcam),

proteoglycan 4 (Cat.#MABT401, Millipore), ephrin A4 (Cat.#PAB3007, Abnova), lysyl oxidase (Cat. #ABT112, Millipore), and CD 31 (Cat.#ab9498, Abcam) were applied overnight at 37 °C with shaking. The next day, corresponding secondary Alexa Flour 488-conjugated or 546-conjugated antibodies (all from Life technology, Carlsbad, CA, USA) were applied for 1 h. Then, samples were counter-stained with 4',6-diamidino2-phenylindole (DAPI) (Life Technology) and mounted with Mowiol.

F-actin staining was used to visualize cell morphology in the 3D hydrogels. The whole hydrogel was incubated with phalloidin-AF488 (Life technologies) for 40 min with shaking at 37 °C. DAPI was used for nuclear counter-staining.

Photographs were taken with an Olympus XC10 camera on an Olympus BX61 fluorescence microscope (Olympus, Japan). Immunofluorescence stainings, including F-actin staining, were independently reproduced twice with the representative Y3-TSPC donor in triplicates. In order to analyze the collagen V, proteoglycan 4, and lysyl oxidase level, an automated quantitative image analysis was conducted using Image J (National Institutes of Health, Bethesda, MD, USA) as described previously [23, 24]. Briefly, the whole image area was manually designated using the 'drawing/selection' tool, then the integrated density, background fluorescence, and area were automatically measured. The corrected total fluorescence (CTF) representing the collagen V, proteoglycan 4, and lysyl oxidase expression were calculated as follows CTF = mean integrated density—(image area × mean background fluorescence). Three samples with four images per group were analyzed. The ephrin A4 positive cells per image were counted manually with 12 images per group.

2.6. Vascular structure formation by HUVECs in the gels

To investigate vascular penetration through the 3D gels, BC or COL I gels with HUVECs at a cell density of 2 × 105 cells/100 μl (2 × 10^3 mm^{-3}) were prepared as described above. The gels, with the same dimensions as before, were loaded with HUVECs and cultured in endothelial cell proliferation medium supplemented with 200 ng ml^{-1} human vascular endothelial growth factor (Cat.#228-11628, TRayBiotech, Norcross, GA) and 200 ng ml^{-1} human fibroblast growth factor basic-2 (Cat.#11018 C, Peprotech, USA) and maintained in a humidified incubator at a constant temperature of 37 °C and 5% CO_2.

Live/dead staining was performed at day 0, 1, and 7 to reveal the cell viability and vascular architecture inside the gels. CD 31 immunofluorescence staining was conducted both in monolayer and 3D gel culture condition to validate the HUVEC phenotype, as described above. The experiments were repeated three times independently.

2.7. Statistical analysis

Data was presented as mean ± standard deviation. Statistical differences between the two groups were determined using unpaired two-tailed non-parametric Student's *t*-test with GraphPad Prism5 software (GraphPad). Differences were considered statistically significant according to values of $^{*}P < 0.05$ and $^{**}P < 0.01$.

3. Results

3.1. Cell survival in BDI hydrogel

Initially, we examined the TSPC-loaded BDI hydrogels for cell survival using live/dead assay. As shown in figure S1 (available online at stacks.iop.org/BMM/13/034107/mmedia), we observed no TSPC spreading and, after 24 h of cultivation, massive cell death occured, indicating that non-functionalized BDI hydrogel does not support the survival of this cell type and that its biocompatibility needed to be improved. Therefore, further experiments were performed to functionalize BDI hydrogel with COL I. Since BDI gel alone causes cell death, which does not permit proper analysis of cell behavior and gene expression, this group was excluded in the following experiments.

3.2. Gel contraction and weight change over time

To understand the dimension stability of gels cultured with TSPCs, contraction analysis was performed with six gels/group from day 0 to day 7. The same gels were measured at each time point. The photos of the contracting gels were taken daily, and the contraction rate was calculated as a percentage of the initial gel area. The results demonstrated that both COL I gel and BC hydrogel contracted over time. However, the contraction rate of the COL I gel was higher than that of the BC hydrogel at all the time points. At day 7, COL I gel was only (13.87 ± 3.321) % of the initial gel area at day 0. At the same time, the area of the BC hydrogel was (74.21 ± 7.123) % of the initial size (figures 2(a), (c)). This indicates that the BC hydrogel dimension was more stable than COL I gel for TSPC expansion.

Weight curves of the hydrogels showed that the weight of both the COL I gel and BC hydrogel increased over the culture time, suggesting cell proliferation and matrix deposition within the hydrogels (figure 2(b)).

3.3. Gel matrix organization and TSPC morphology

To observe the gel matrix organization, immunostaining with anti-collagen type I was performed. COL I gel was strongly positive (figures 3(a1), (a2), (b1) and (b4)). In the BC hydrogel, the COL fibers were distributed homogeneously in the matrix (figures 3(a3), (a4), (b7) and (b10)). Next, after 3 days culture with TSPC, actin staining was conducted to demonstrate the cell morphology and formation of stress fibers. The results showed that TSPCs stretched well in COL I gel with classical

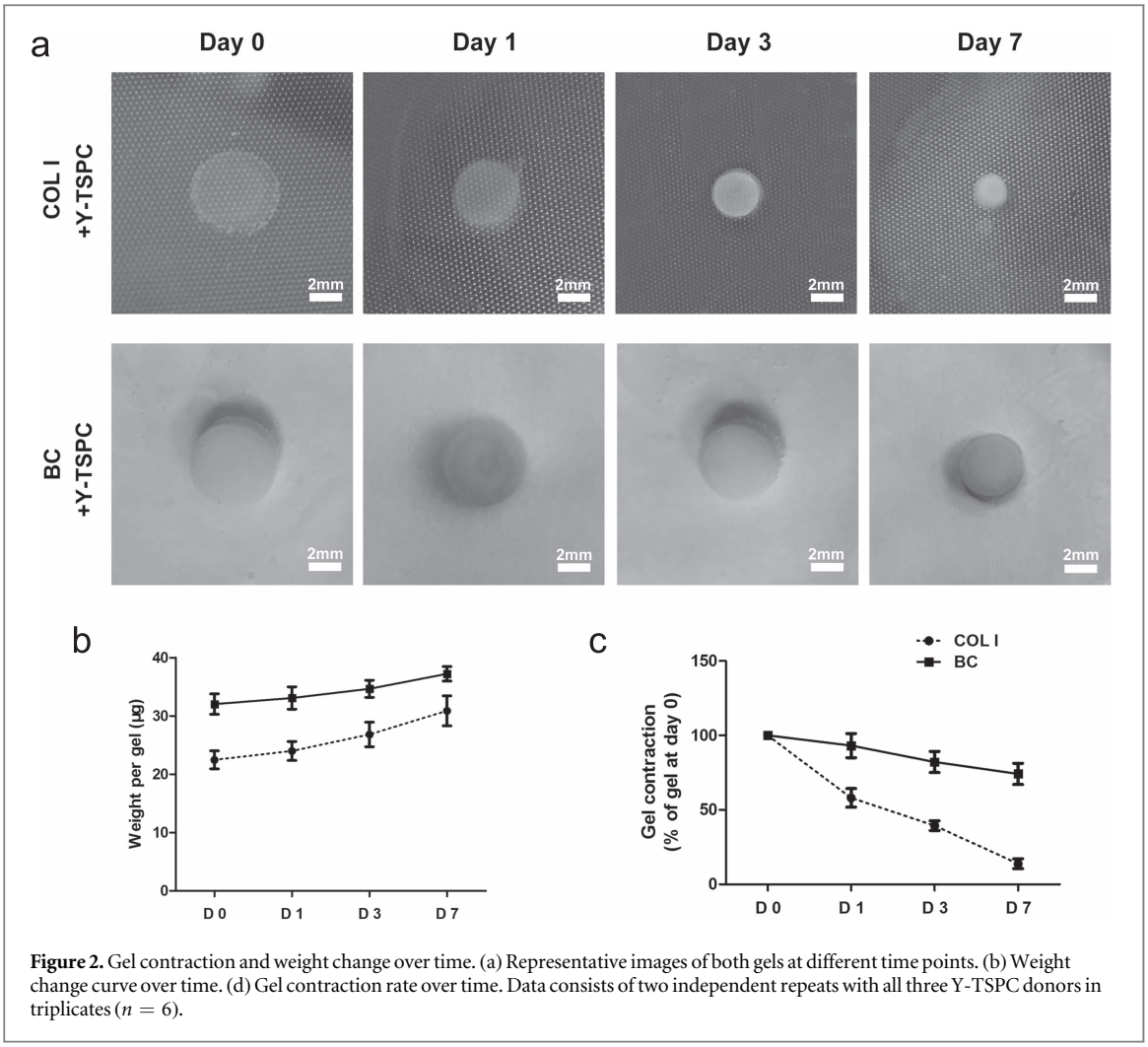

Figure 2. Gel contraction and weight change over time. (a) Representative images of both gels at different time points. (b) Weight change curve over time. (d) Gel contraction rate over time. Data consists of two independent repeats with all three Y-TSPC donors in triplicates ($n = 6$).

spindle cell shapes (figures 3(b2) and (b5)) and membranous protrusions (white arrows in figure 3(b5)). Similar cell morphologies were also found in the BC hydrogel (figures 3(b8) and (b11)). The formation of stress fibers was observed on both materials (higher magnification insets in figures (b5) and (b11)).

3.4. TSPC viability, elongation, apoptosis, and proliferation

Cell viability, apoptosis, and proliferation in the gels were examined by live/dead staining, JC-1 staining, DNA quantification, and cell metabolic assay at different time points. The cells distributed evenly in both gels, and most of the TSPCs remained viable (green color) in COL I and the BC hydrogel immediately after encapsulation. From day 1, the TSPC tended to stretch, and dead cells (red color) were found only occasionally in both gels. Even at day 7, most of the TSPCs stayed alive in the gels. There was an apparent increase in cell number observed from day 0 to day 7 (figures 4, S2). Since the TSPCs were well revealed at each time point with the calcein dye from the live/dead assay, this staining was used to evaluate cell elongation by calculation of cell aspect ratio (figure 4(b)) in the experimental time course. Figure 4(c) shows clear cell elongation at day 3, but no significant difference in cell aspect ratio between TSPCs cultivated in COL I or BC hydrogel at each time point (figure 4(c)).

This cell growth trend was further validated by DNA quantification. The results showed that the total DNA content increased over time in both gels, and there was no significant difference between the COL I gel and BC hydrogel after 3 days in culture. However, the DNA content in the COL I gel was higher than that in the BC hydrogel after 7 days (figure 5(c)).

JC-1 staining revealed that TSPCs survived in both gels over time, and apoptotic cells (green color) were observed only occasionally during this period (figures 5(a), S2). This result was consistent with live/dead staining. Resazurin assay indicated that TSPC expanded in the gels with high metabolic activity, and there was no significant difference between the two gels (figure 5(b)).

In summary, our data revealed that the BC hydrogel supported TSPC survival, proliferation, and metabolic activity with satisfactory biocompatibility.

3.5. Gene expression profile

RealTime PCR Ready Custom designed plates with 48 genes in total related to tenogenic, COL cross-linking, and lineage gene markers were performed to reveal the

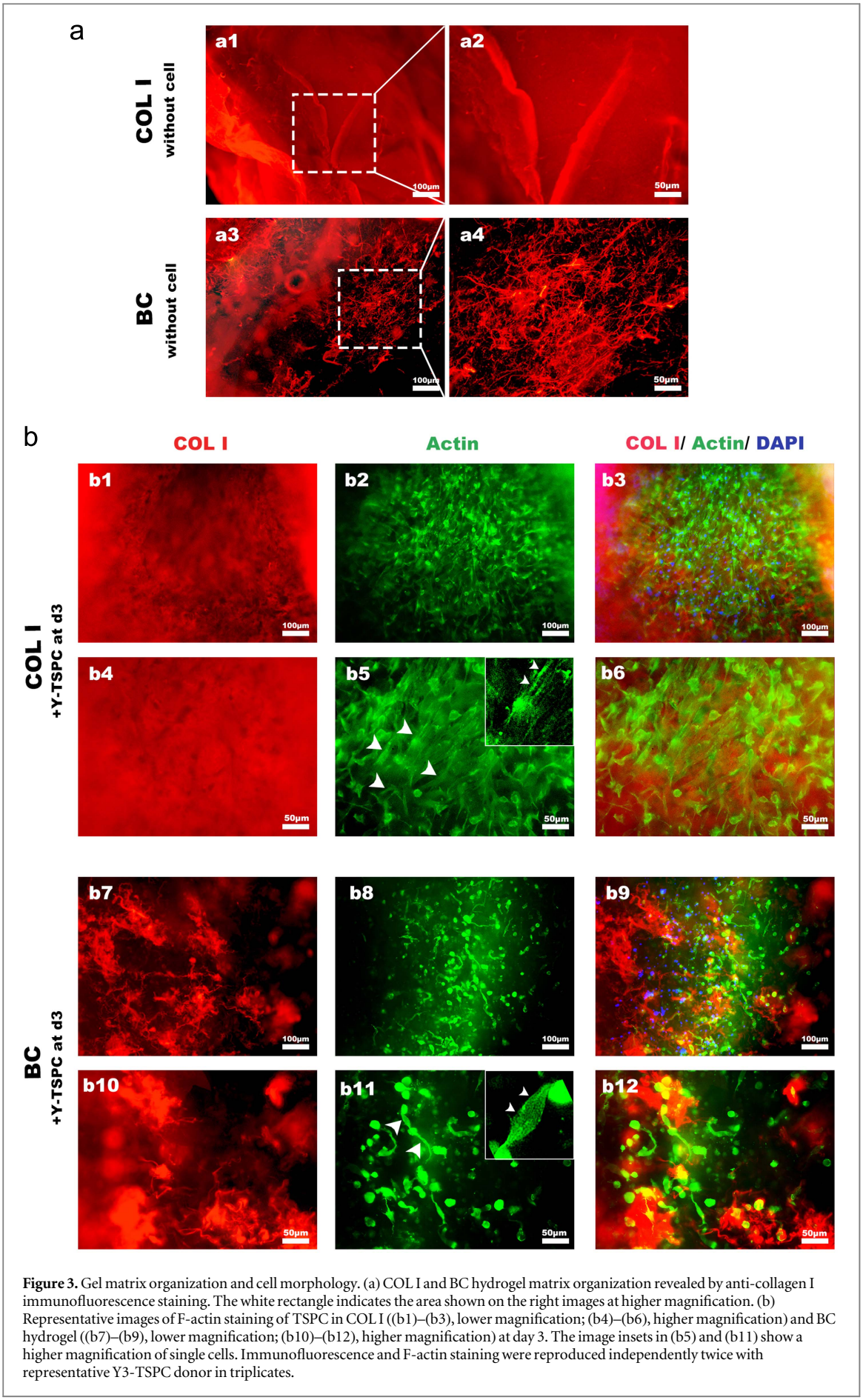

Figure 3. Gel matrix organization and cell morphology. (a) COL I and BC hydrogel matrix organization revealed by anti-collagen I immunofluorescence staining. The white rectangle indicates the area shown on the right images at higher magnification. (b) Representative images of F-actin staining of TSPC in COL I ((b1)–(b3), lower magnification; (b4)–(b6), higher magnification) and BC hydrogel ((b7)–(b9), lower magnification; (b10)–(b12), higher magnification) at day 3. The image insets in (b5) and (b11) show a higher magnification of single cells. Immunofluorescence and F-actin staining were reproduced independently twice with representative Y3-TSPC donor in triplicates.

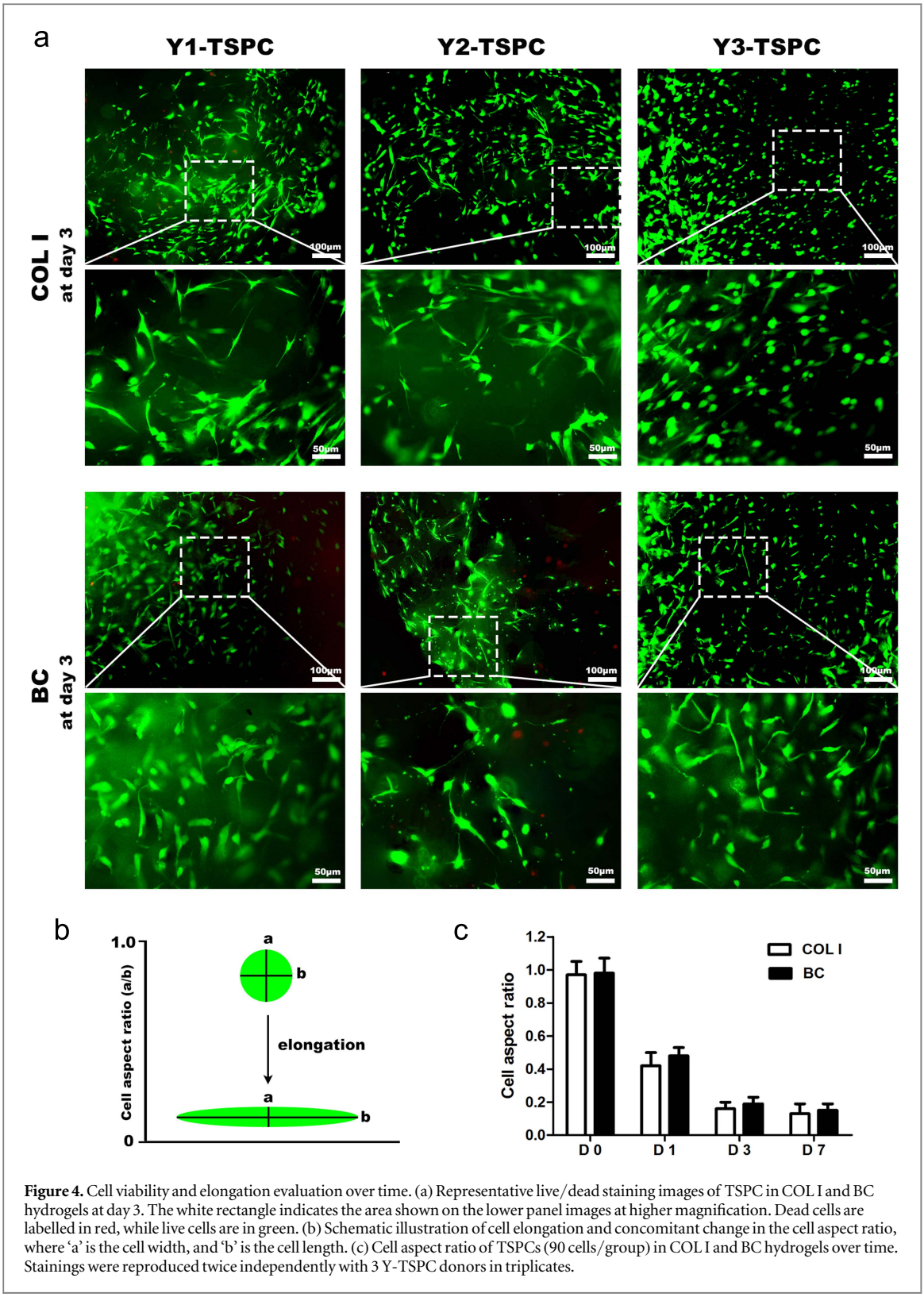

Figure 4. Cell viability and elongation evaluation over time. (a) Representative live/dead staining images of TSPC in COL I and BC hydrogels at day 3. The white rectangle indicates the area shown on the lower panel images at higher magnification. Dead cells are labelled in red, while live cells are in green. (b) Schematic illustration of cell elongation and concomitant change in the cell aspect ratio, where 'a' is the cell width, and 'b' is the cell length. (c) Cell aspect ratio of TSPCs (90 cells/group) in COL I and BC hydrogels over time. Stainings were reproduced twice independently with 3 Y-TSPC donors in triplicates.

gene expression profile of TSPC in both gels at day 3. The results showed that there was no significant difference in the expression level of most of the tendon-related matrix and transcription factor genes, such as asporin (ASPN), biglycan (BCN), decorin (DCN), tenascin C (TNC), COL1A1, COL3A1, scleraxis (SCX), Mohawk (MKX), eyes absent homolog 1 (EYA1), and eyes absent homolog 2 (EYA2) between TSPCs grown in COL I or BC hydrogel. However, several genes, such as thrombospondin 2 (THBS2), early growth response 2 (EGR2), COL5A1, ephrin receptor A4 (EPHA4), and transglutaminase 2 (TGM2) were down-regulated in the BC hydrogel. At the same time, some genes, such as proteoglycan 4 (PRG-4), early growth response 1 (EGR1), and lysyl oxidase (LOX) were up-regulated in the BC hydrogel (figure 6). As for the lineage

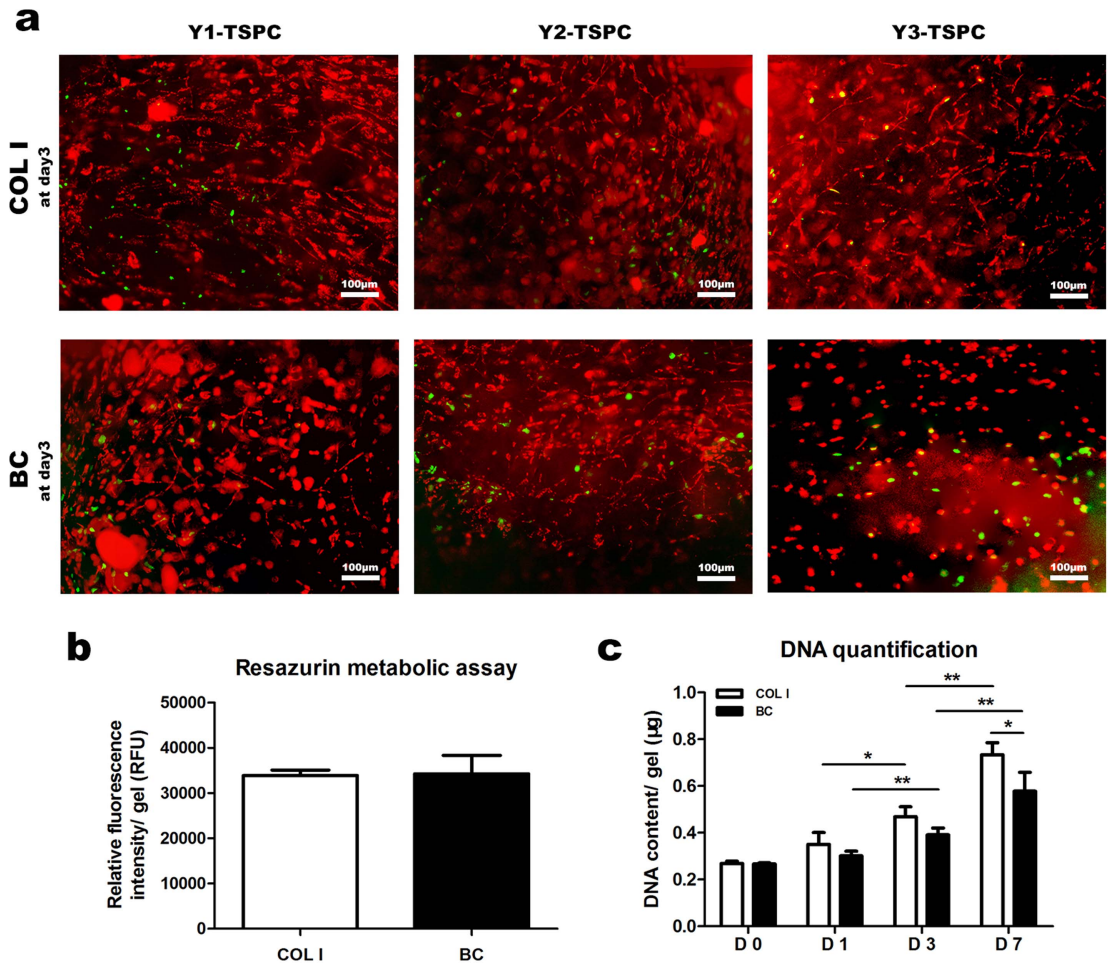

Figure 5. Cell apoptosis and proliferation assays. (a) Representative JC-1 staining images of TSPC in COL I and BC hydrogel at day 3. Red represents the live cells and green represents the apoptotic cells. (b) Resazurin metabolic assay at day 3. (c) DNA quantification at different time points. Quantitative data consists of two independent repeats with all three Y-TSPC donors in triplicates ($n = 6$, $^{*}p < 0.05$, $^{**}p < 0.01$).

markers (chondrogenic, osteogenic, adipogenic, myogenic, embryonic), these were not expressed or at a very low level (with Ct values around 40) and therefore not involved in fold change calculation. In general, the gene expression profile of the TSPCs in the BC hydrogel was highly comparable with the cultivated cells in COL I gel.

3.6. Protein expression of collagen V, proteoglycan 4, lysyl oxidase, and ephrin A4

Promoted by the TSPC gene expression data, we then performed immunofluorescence staining to show the protein deposition in the matrix of both gels. The results showed that there was a greater protein accumulation of proteoglycan 4 and lysyl oxidase in the BC hydrogel, while more ephrin A4 positive cells were observed in COL I gel (figure 7) which together was consistent with the qPCR data. However, on the protein level, no significant difference of COL V deposition was detected between the two hydrogels.

3.7. Vascular permeability

Capillary-like formation and penetration is very critical during the early stages of tendon repair for transporting nutrition and immune regulatory cells to the injury site [5, 25]. Thus, we investigated whether the gels support angiogenesis. The HUVEC phenotype was validated by CD 31 staining both in monolayer and 3D gel culture condition (figures 8(a), (c)). Live/dead staining showed that most of the HUVECs were viable in both gels at day 1. At day 7, many capillary-like structures were observed in the COL I and BC hydrogels (figure 8(b)). Hence, our results indicated that the BC hydrogel supported angiogenesis by HUVECs.

4. Discussion

Current therapeutic options for tendon injury have limited clinical outcomes owing to the poor self-repair capacity of tendon tissue [6, 26]. Thermosensitive hydrogels have been extensively studied as a promising alternative stem cell delivery system for tissue engineering-based therapeutical strategies [27]. This study developed an injectable synthetic/natural hybrid BC hydrogel as a delivery carrier of tendon stem/progenitor cells for tendon tissue engineering. The BC hydrogel

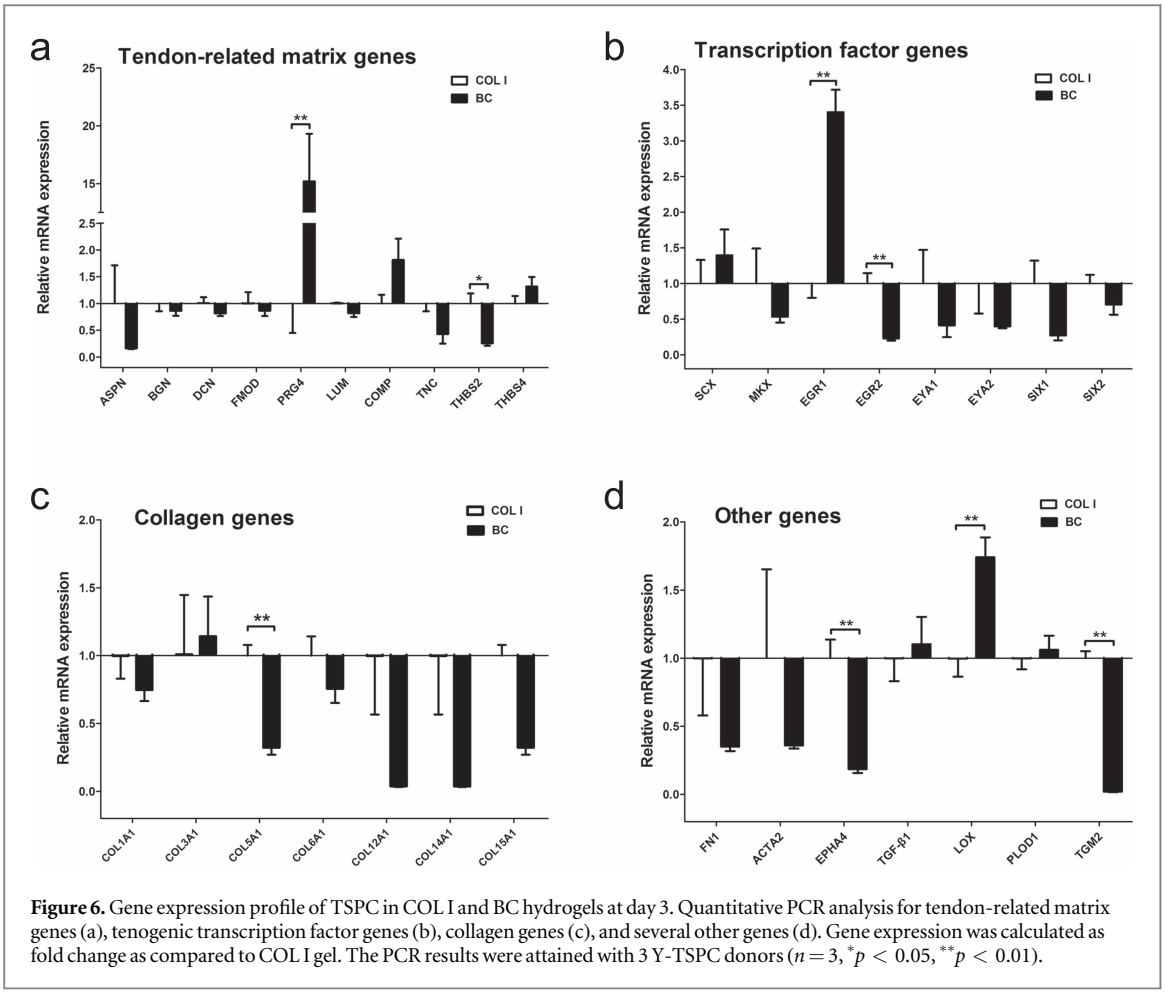

Figure 6. Gene expression profile of TSPC in COL I and BC hydrogels at day 3. Quantitative PCR analysis for tendon-related matrix genes (a), tenogenic transcription factor genes (b), collagen genes (c), and several other genes (d). Gene expression was calculated as fold change as compared to COL I gel. The PCR results were attained with 3 Y-TSPC donors ($n = 3$, $^{*}p < 0.05$, $^{**}p < 0.01$).

exhibited a sol-gel transition around 25 °C as a function of its pluronic content, and showed great dimension stability and biocompatibility. Rheological measurements which reflect the mechanical properties of materials in terms of storage and loss moduli have been performed for BDI and COL I hydrogels in previous publications [16]. The material storage modulus is related to its ability to return energy, representing elastic energy, while the loss modulus reflects the material's propensity to lose energy, representing dissipative energy [28]. McBane *et al* [29] reported that the combination of chitosan and COL I results in stronger mechanical properties than pure COL I hydrogel. Baniasadi *et al* [28] showed that the addition of COL I to alginate hydrogel substantially improved the rheological and indentation properties of the composite hydrogel. The BDI hydrogel showed a storage modulus of 0.3 kPa at 37 °C [16] while COL I hydrogel with a concentration of 6 mg ml^{-1} had a storage modulus of 0.25 kPa [28]. In our study, 20 percent volume of 4.75 mg ml^{-1} COL I was used to functionalize the BDI hydrogel, resulting in a final concentration similar to that of the COL I hydrogel, which was expected to be comparable if not even superior to the mechanical properties of the BC hydrogel. However, follow up investigations should examine precisely the rheological features of the novel BC hydrogel.

To investigate the applicability of the BC hydrogel as a cell delivery carrier for tendon tissue engineering, *in vitro* culture of clinically relevant human tendon stem/progenitor cells cultivated in a 3D gel environment was conducted. Initially, we examined BDI alone and showed that when non-functionalized, it is not biocompatible for TSPCs as it induced massive cell death, even after short-term cultivation. This finding is in line with previous studies. For example, Khattak *et al* [18] reported no evident cell proliferation for three different cell lines (HepG2: human liver carcinoma cells, HMEC-1: endothelial, and L6: muscle) encapsulated in pluronic F127 hydrogel, but complete cell death over a period of 5 days. Therefore, in our study, we used only a COL I gel as a control group. Numerous studies have shown that a COL I gel provides a 3D environment with great compatibility and excellent cell adhesion [20, 30, 31]. Matrix organization analysis revealed a homogeneous distribution of COL I in the BC hydrogel. Furthermore, phalloidin-based visualization of F-actin demonstrated that TSPCs were stretched well in COL I gel with classical spindle cell shapes, and similar cell morphologies were also found in the BC hydrogel. Next, cell shape analysis via calculation of cell aspect ratio revealed clear cell elongation at day 3 with no significant differences in the cell aspect ratio between TSPCs cultivated in either

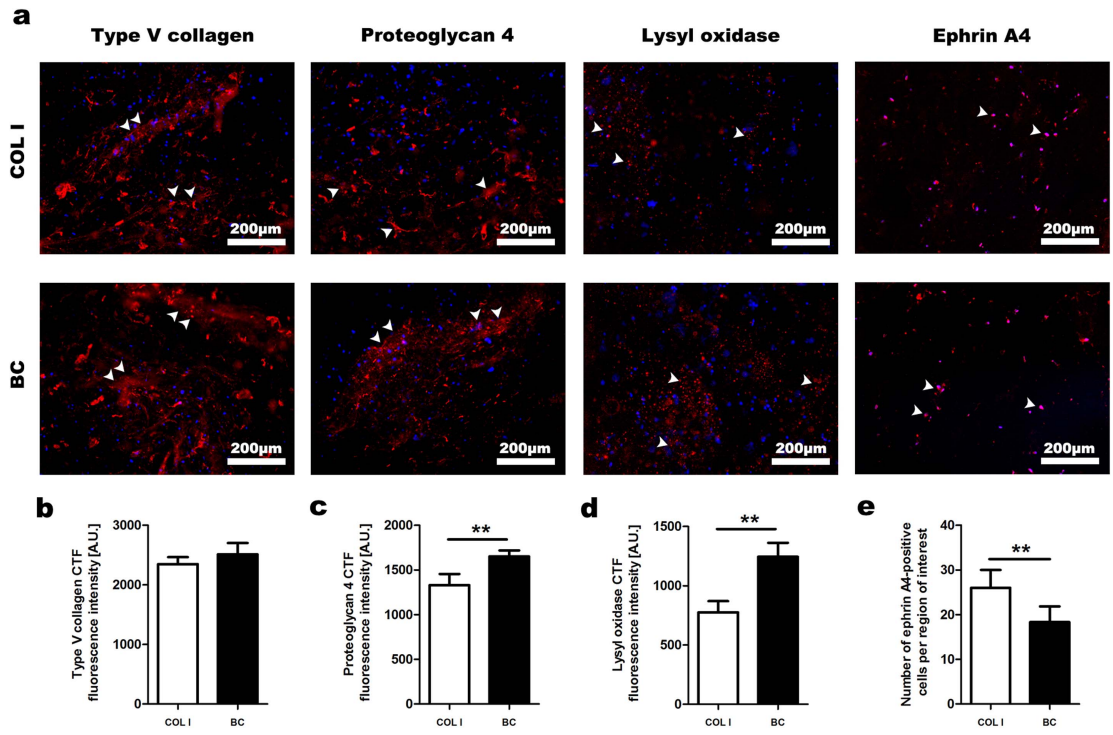

Figure 7. Protein expression analyses of collagen V, proteoglycan 4, lysyl oxidase, and ephrin A4. (a) Representative images of immunofluorescence staining with anti-type V collagen, proteoglycan 4, lysyl oxidase, and ephrin A4. (b)–(e) The type V collagen, proteoglycan 4, lysyl oxidase expression were quantified by automated digital image analyses, and ephrin A4 positive cells were counted manually. Stainings were reproduced twice independently with the representative Y3-TSPC donor in triplicates, and in the quantitative analysis three samples with four images per group were analysed ($^{**}p < 0.01$).

of the hydrogels during the cultivation time course. Gel contraction assay demonstrated that both COL I and BC hydrogels were contracted over time. However, the contraction rate of COL I gel was much higher than that of the BC hydrogel at all of the studied time points. This indicates that the BC hydrogel dimension was more stable than COL gel during TSPC cultivation and expansion. Live/dead staining showed that the TSPCs were encapsulated homogeneously and the majority of the cells stayed alive in both hydrogels over extended culture periods. In addition, there was an apparent increase in cell numbers from day 0 to day 7, which was further validated by DNA quantification. Resazurin assay and JC-1 staining indicated that both hydrogels supported high TSPC metabolic activity and did not induce apparent cell apoptosis, respectively. In general, these findings indicate that the BC hydrogel supported TSPC survival, proliferation, and metabolic activity in a manner comparable to COL I.

Biomaterials provide a micro-environment for cell growth and can influence stemness and cell fate [32, 33]. Therefore, it is critical to investigate how biomaterials influence the cellular gene expression profile. However, many studies have reported very limited gene expression data. Firstly, the TSPC basic gene expression profile in monolayer culture has been investigated and reported previously by Kohler *et al* [11]. Here, we performed a comprehensive gene expression analysis of TSPC grown in COL I or BC hydrogels, including lineage-specific (chondrogenic, osteogenic, adipogenic, myogenic, embryonic) and multiple tendon-related gene markers. When maintained in a 3D hydrogel environment, the TSPC phenotype was stable and, apart from few significantly differentially expressed genes, most of the tendon-related matrix and transcription factor genes had comparable levels in the two hydrogel types. Tenomodulin (Tnmd), a gene abundantly expressed in tendons and ligaments [34–38], has been shown to play important roles in regulating TSPC functions as well as COL I fibrils during tendon development and upon mechanical load. Loss of Tnmd expression in mice led to pathological thickening of COL I fibrils [36, 37]. In our study, Tnmd expression was not detectable on an mRNA level in both hydrogels, which is consistent with previous results demonstrating that *in vitro* culturing of human TSPC leads to a rapid loss of Tnmd mRNA [11, 37]. It is also important to note that the down-regulation of some genes in the BC hydrogel seemed to be compensated by the up-regulation of genes with a similar function. As EGR2 (a tendon-related transcription factor) down-regulated, its homolog EGR1 up-regulated in the BC hydrogel. EGR1 has been reported to control divergent cellular responses; however, genetic knock-out in mice for EGR1 shows no overt phenotype due to the activation of redundant mechanisms of EGR2–4 that compensate for the loss of the EGR1 function [39]. TGM2 (a COL

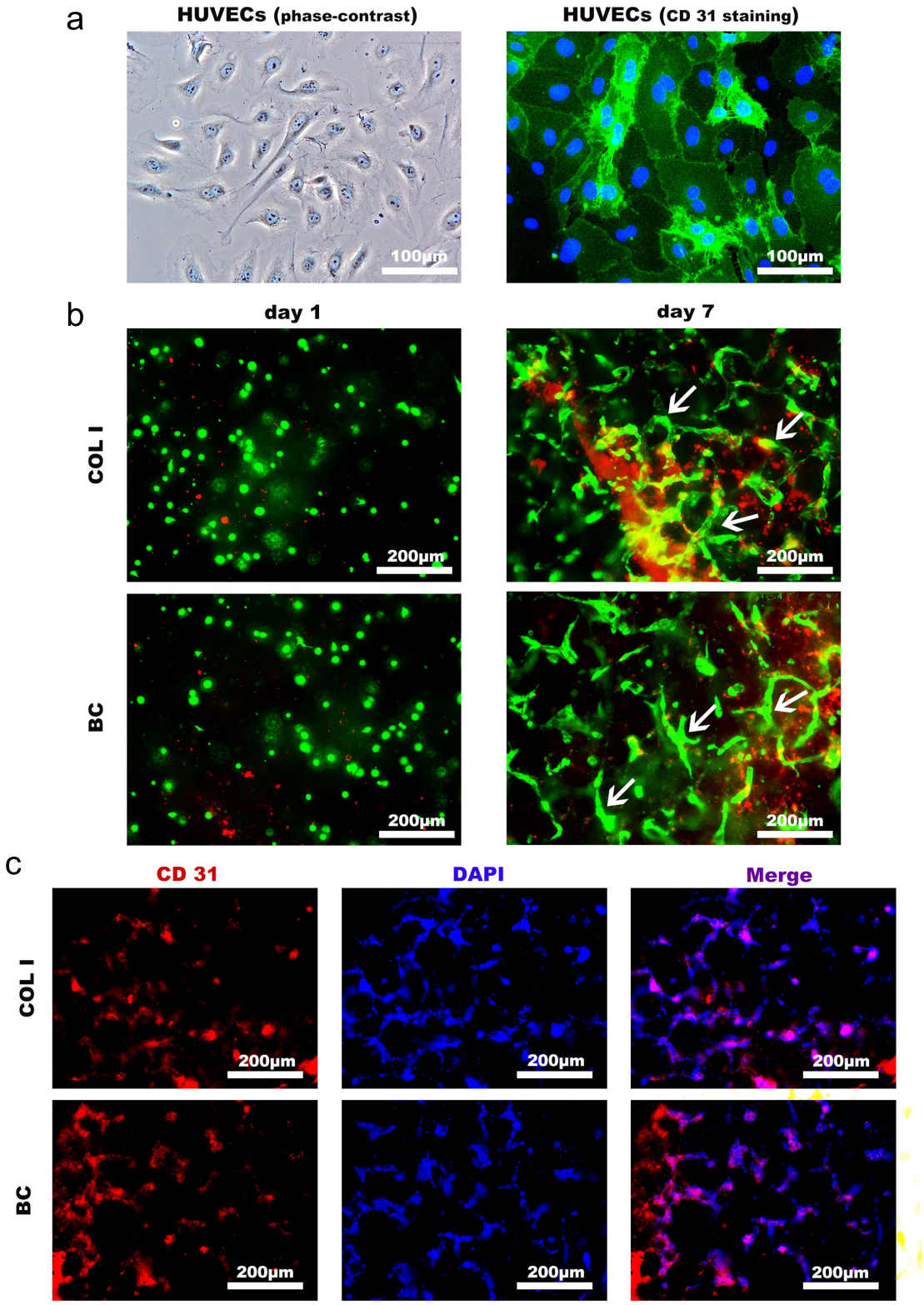

Figure 8. Capillary-like formation by HUVECs. (a) Representative images of phase contrast and anti-CD 31 staining of monolayer HUVECs. (b) Representative live/dead staining of HUVECs in COL I and BC hydrogel at day 1 and day 7. (c) Anti-CD 31 staining of HUVECs in the gels. Stainings were reproduced three times independently with HUVECs in triplicates.

cross-linking gene) was down-regulated, whilst another COL cross-linking enzyme, LOX, was up-regulated in the BC hydrogel. How genes that have a similar gene function will be differentially expressed is difficult to predict as it is very cell/tissue type-specific. Therefore, the exact signaling pathways triggered by a dysregulated gene expression have to be further carefully investigated. Regarding the lineage-specific markers, most of the genes were not expressed or detected at a very low level. In conclusion, the gene expression profile of TSPCs in the BC hydrogel was highly comparable to that of COL I gel. We next performed

immunofluorescence stainings to validate the protein expression of four differentially expressed genes in both hydrogels. The protein expression of EPHA4 (a receptor tyrosine kinases that mediates short-range cell–cell communication [13]), PRG4 (also known as lubricin—a proteoglycan that aids smooth gliding of tendons [5]) and LOX [37]) in the BC hydrogel was consistent with the qPCR data. In the case of proteoglycan 4 gene and protein expression, qPCR results revealed an upregulation of approximately 15 fold of the mRNA levels when cells were cultivated in the BC hydrogel, while densitometric protein analyses showed significant but lower protein upregulation. COL5 is one of the tendon matrix protein components, which plays a critical role in regulating COL I fibrillogenesis and matrix organization [40]. COL V-deficient mice in tendons and ligaments exhibit abnormal COL I fiber organization and structure with decreased COL I fibril number and increased fibril diameters [41]. Our PCR results showed higher COL5A1 mRNA levels in COL I than BC hydrogel; however, no significant difference of COL5 accumulation was detected by immunostainings between both gel types. COL expression is complexly regulated in many steps during transcription and translation as well as degradation. Thus, mRNA expression levels are predictable but not necessarily reflected at the protein level [42]. Therefore, it will be important to perform additional quantitative analyses, such as western blotting or ELISA in follow-up studies.

During the tendon repair process, especially in the early stage, blood supply is essential to transport nutrition and immune cells with regulatory and defensive functions to the injury site [5, 25]. Thus, it is very important that the *in vivo* implanted biomaterials can be penetrated by vessels. Our study revealed that both hydrogels supported HUVEC survival and capillary-like structure formation.

The critical limitation of the hydrogels is that they cannot provide, in a full tendon tear scenario, the desired biomechanical strength and tissue continuity [43]. However, the clinical translation of this thermosensitive BC hydrogel can be specialized for cells, growth factors, or drug delivery in partial tendon lesions, contained tendon defects, injection underneath tendon sheets, or to enhance conservative treated tendon injuries. In the future, we plan to investigate the performance of this thermosensitive BC hydrogel combined with TSPCs in a clinical relevant tendon injury model which we established previously [6].

5. Conclusion

This study developed a thermosensitive BC hydrogel as an injectable delivery carrier of TSPCs for tendon tissue engineering. The BC hydrogel exhibited a sol-gel transition around 25 °C with satisfactory dimension stability. Moreover, the BC hydrogel supported TSPC survival, proliferation, and metabolic activity over a long period of time. In the BC hydrogel, TSPCs exhibited adequate cell morphology, and their gene expression profile was comparable to COL I gel. Finally, the BC hydrogel supported HUVEC capillary-like formation, thus suggesting that the hydrogel matrix is permeable for vessels. Taken together, the BC hydrogel combined with reparative cells offers a great application potential for minimally invasive treatment of partial tendon lesions, contained tendon defects, underneath tendon sheets, or conservative treated tendon injury therapy.

Acknowledgments

H Y is grateful for the support from the China Scholarship Council (CSC) (Grant No. 201606200072). The authors thank Daniela Drenkard for valuable technical assistance and Brigitta Hauer for providing the HUVECs.

ORCID iDs

Denitsa Docheva https://orcid.org/0000-0002-7588-1290

References

[1] Lantto I, Heikkinen J, Flinkkila T, Ohtonen P and Leppilahti J 2015 Epidemiology of Achilles tendon ruptures: increasing incidence over a 33-year period *Scand. J. Med. Sci. Sports* **25** e133–8

[2] Zhou B, Zhou Y and Tang K 2014 An overview of structure, mechanical properties, and treatment for age-related tendinopathy *J. Nutr. Health Aging* **18** 441–8

[3] Rees J D, Wilson A M and Wolman R L 2006 Current concepts in the management of tendon disorders *Rheumatology* **45** 508–21

[4] Urwin M, Symmons D, Allison T, Brammah T, Busby H, Roxby M, Simmons A and Williams G 1998 Estimating the burden of musculoskeletal disorders in the community: the comparative prevalence of symptoms at different anatomical sites, and the relation to social deprivation *Ann. Rheum. Dis.* **57** 649–55

[5] Docheva D, Muller S A, Majewski M and Evans C H 2015 Biologics for tendon repair *Adv. Drug. Deliv. Rev.* **84** 222–39

[6] Hsieh C F, Alberton P, Loffredo-Verde E, Volkmer E, Pietschmann M, Muller P, Schieker M and Docheva D 2016 Scaffold-free Scleraxis-programmed tendon progenitors aid in significantly enhanced repair of full-size Achilles tendon rupture *Nanomedicine* **11** 1153–67

[7] Sajovic M, Strahovnik A, Dernovsek M Z and Skaza K 2011 Quality of life and clinical outcome comparison of semitendinosus and gracilis tendon versus patellar tendon autografts for anterior cruciate ligament reconstruction: an 11-year follow-up of a randomized controlled trial *Am. J. Sports Med.* **39** 2161–9

[8] Snedeker J G and Foolen J 2017 Tendon injury and repair—a perspective on the basic mechanisms of tendon disease and future clinical therapy *Acta Biomater.* **63** 18–36

[9] Bi Y *et al* 2007 Identification of tendon stem/progenitor cells and the role of the extracellular matrix in their niche *Nat. Med.* **13** 1219–27

[10] Zhang X, Lin Y C, Rui Y F, Xu H L, Chen H, Wang C and Teng G J 2016 Therapeutic roles of tendon stem/progenitor cells in tendinopathy *Stem Cells Int.* **2016** 4076578

[11] Kohler J *et al* 2013 Uncovering the cellular and molecular changes in tendon stem/progenitor cells attributed to tendon aging and degeneration *Aging Cell* **12** 988–99
[12] Popov C, Burggraf M, Kreja L, Ignatius A, Schieker M and Docheva D 2015 Mechanical stimulation of human tendon stem/progenitor cells results in upregulation of matrix proteins, integrins and MMPs, and activation of p38 and ERK1/2 kinases *BMC Mol. Biol.* **16** 6
[13] Popov C, Kohler J and Docheva D 2015 Activation of EphA4 and EphB2 reverse signaling restores the age-associated reduction of self-renewal, migration, and actin turnover in human tendon stem/progenitor cells *Front. Aging Neurosci.* **7** 246
[14] Naahidi S, Jafari M, Logan M, Wang Y, Yuan Y, Bae H, Dixon B and Chen P 2017 Biocompatibility of hydrogel-based scaffolds for tissue engineering applications *Biotechnol. Adv.* **35** 530–44
[15] Park K M, Lee S Y, Joung Y K, Na J S, Lee M C and Park K D 2009 Thermosensitive chitosan-Pluronic hydrogel as an injectable cell delivery carrier for cartilage regeneration *Acta Biomater.* **5** 1956–65
[16] Volkmer E *et al* 2013 Poloxamer-based hydrogels hardening at body core temperature as carriers for cell based therapies: *in vitro* and *in vivo* analysis *J. Mater. Sci., Mater. Med.* **24** 2223–34
[17] Fedorovich N E, Swennen I, Girones J, Moroni L, Van Blitterswijk C A, Schacht E, Alblas J and Dhert W J 2009 Evaluation of photocrosslinked Lutrol hydrogel for tissue printing applications *Biomacromolecules* **10** 1689–96
[18] Khattak S F, Bhatia S R and Roberts S C 2005 Pluronic F127 as a cell encapsulation material: utilization of membrane-stabilizing agents *Tissue Eng.* **11** 974–83
[19] Hwang Y S, Chiang P R, Hong W H, Chiao C C, Chu I M, Hsiue G H and Shen C R 2013 Study *in vivo* intraocular biocompatibility of *in situ* gelation hydrogels: poly(2-ethyl oxazoline)-block-poly(epsilon-caprolactone)-block-poly(2-ethyl oxazoline) copolymer, matrigel and pluronic F127 *PLoS One* **8** e67495
[20] Awad H A, Butler D L, Harris M T, Ibrahim R E, Wu Y, Young R G, Kadiyala S and Boivin G P 2000 *In vitro* characterization of mesenchymal stem cell-seeded collagen scaffolds for tendon repair: effects of initial seeding density on contraction kinetics *J. Biomed. Mater. Res.* **51** 233–40
[21] Yang C H, Wang M X, Haider H, Yang J H, Sun J Y, Chen Y M, Zhou J and Suo Z 2013 Strengthening alginate/polyacrylamide hydrogels using various multivalent cations *ACS Appl. Mater. Interfaces* **5** 10418–22
[22] Popov C, Radic T, Haasters F, Prall W C, Aszodi A, Gullberg D, Schieker M and Docheva D 2011 Integrins $\alpha2\beta1$ and $\alpha11\beta1$ regulate the survival of mesenchymal stem cells on collagen I *Cell Death Dis.* **2** e186
[23] Lin D, Alberton P, Caceres M D, Volkmer E, Schieker M and Docheva D 2017 Tenomodulin is essential for prevention of adipocyte accumulation and fibrovascular scar formation during early tendon healing *Cell Death Dis.* **8** e3116
[24] Hsieh C F, Alberton P, Loffredo-Verde E, Volkmer E, Pietschmann M, Muller P E, Schieker M and Docheva D 2016 Periodontal ligament cells as alternative source for cell-based therapy of tendon injuries: *in vivo* study of full-size Achilles tendon defect in a rat model *Eur. Cell Mater.* **32** 228–40
[25] Kajikawa Y *et al* 2007 GFP chimeric models exhibited a biphasic pattern of mesenchymal cell invasion in tendon healing *J. Cell. Physiol.* **210** 684–91
[26] Webb W R, Dale T P, Lomas A J, Zeng G, Wimpenny I, El Haj A J, Forsyth N R and Chen G Q 2013 The application of poly(3-hydroxybutyrate-co-3-hydroxyhexanoate) scaffolds for tendon repair in the rat model *Biomaterials* **34** 6683–94
[27] Breidenbach A P, Dyment N A, Lu Y, Rao M, Shearn J T, Rowe D W, Kadler K E and Butler D L 2015 Fibrin gels exhibit improved biological, structural, and mechanical properties compared with collagen gels in cell-based tendon tissue-engineered constructs *Tissue Eng. Part* A **21** 438–50
[28] Baniasadi M and Minary-Jolandan M 2015 Alginate-collagen fibril composite hydrogel *Materials* **8** 799–814
[29] Mcbane J E, Vulesevic B, Padavan D T, Mcewan K A, Korbutt G S and Suuronen E J 2013 Evaluation of a collagen-chitosan hydrogel for potential use as a pro-angiogenic site for islet transplantation *PLoS One* **8** e77538
[30] Abraham T, Carthy J and Mcmanus B 2010 Collagen matrix remodeling in 3-dimensional cellular space resolved using second harmonic generation and multiphoton excitation fluorescence *J. Struct. Biol.* **169** 36–44
[31] Duncan N A, Bruehlmann S B, Hunter C J, Shao X and Kelly E J 2014 *In situ* cell-matrix mechanics in tendon fascicles and seeded collagen gels: implications for the multiscale design of biomaterials *Comput. Methods Biomech. Biomed. Engin.* **17** 39–47
[32] Chaudhuri O *et al* 2016 Hydrogels with tunable stress relaxation regulate stem cell fate and activity *Nat. Mater.* **15** 326–34
[33] Haugh M G and Heilshorn S C 2016 Integrating concepts of material mechanics, ligand chemistry, dimensionality and degradation to control differentiation of mesenchymal stem cells *Curr. Opin. Solid State Mater. Sci.* **20** 171–9
[34] Brandau O, Meindl A, Fassler R and Aszodi A 2001 A novel gene, tendin, is strongly expressed in tendons and ligaments and shows high homology with chondromodulin-I *Dev. Dyn.* **221** 72–80
[35] Shukunami C, Oshima Y and Hiraki Y 2001 Molecular cloning of tenomodulin, a novel chondromodulin-I related gene *Biochem. Biophys. Res. Commun.* **280** 1323–7
[36] Docheva D, Hunziker E B, Fassler R and Brandau O 2005 Tenomodulin is necessary for tenocyte proliferation and tendon maturation *Mol. Cell. Biol.* **25** 699–705
[37] Dex S *et al* 2017 Tenomodulin is required for tendon endurance running and collagen I fibril adaptation to mechanical load *EBioMedicine* **20** 240–54
[38] Dex S, Lin D, Shukunami C and Docheva D 2016 Tenogenic modulating insider factor: systematic assessment on the functions of tenomodulin gene *Gene* **587** 1–17
[39] Van Den Akker G G *et al* 2016 EGR1 controls divergent cellular responses of distinctive nucleus pulposus cell types *BMC Musculoskelet. Disord.* **17** 124
[40] Wenstrup R J, Florer J B, Brunskill E W, Bell S M, Chervoneva I and Birk D E 2004 Type V collagen controls the initiation of collagen fibril assembly *J. Biol. Chem.* **279** 53331–7
[41] Sun M, Connizzo B K, Adams S M, Freedman B R, Wenstrup R J, Soslowsky L J and Birk D E 2015 Targeted deletion of collagen V in tendons and ligaments results in a classic Ehlers-Danlos syndrome joint phenotype *Am. J. Pathol.* **185** 1436–47
[42] Vogel C and Marcotte E M 2012 Insights into the regulation of protein abundance from proteomic and transcriptomic analyses *Nat. Rev. Genet.* **13** 227–32
[43] Hoffman A S 2002 Hydrogels for biomedical applications *Adv. Drug. Deliv. Rev.* **54** 3–12